Numerical and Experimental Investigation of a Non-Newtonian Flow in a Collapsed Elastic Tube

Franz X. Tanner[1]*, Abdallah A. Al-Habahbeh[1], Kathleen A. Feigl[1], Samsun Nahar[2], Shaik A. K. Jeelani[2], William R. Case[2], and Erich J. Windhab[2]

[1] Department of Mathematical Sciences, Michigan Technological University, Houghton, MI 49931-1295, USA
[2] Laboratory of Food Process Engineering, ETH Zurich, 8092 Zurich, Switzerland

*Corresponding author: tanner@mtu.edu

Received: 16.7.2012, Final version: 10.10.2012

Abstract:
Simulations are performed to investigate the flow of a shear-thinning, non-Newtonian fluid in a collapsed elastic tube and comparisons are made with experimental data. The fluid is modeled by means of the Bird- Carreau viscosity law. The computational domain of the deformed tube is constructed from data obtained via computer tomography imaging. Comparison of the computed velocity fields with the ultrasound Doppler velocity profile measurements show good agreement, as does the adjusted pressure drop along the tube's axis. Analysis of the shear rates show that the shear-thinning effect of the fluid becomes relevant in the crosssections with the biggest deformation. In fact, the maximum shear rate is about a factor of thirty larger than its corresponding maximum value in the undeformed tube, and the viscosity is reduced by a factor of two. The effect of the shear-thinning behavior has also been compared with identical simulations carried out for a Newtonian fluid.

Zusammenfassung:
Es werden Ergebnisse von Simulationen vorgestellt, um das Fließen eines scherverdünnenden, nicht-Newtonschen Fluids in einer kollabierten elastischen Röhre zu untersuchen. Zusätzlich werden Vergleiche mit experimentellen Daten gemacht. Das Fluid wird durch ein Bird-Carreau-Viskositätsgesetz modelliert. In der Simulation wird das Gitter für die deformierte Röhre aus Daten, die mittels Computer-Tomographie gewonnen wurden, konstruiert. Der Vergleich des berechneten Geschwindigkeitsfeldes mit den Ultraschall-Dopplergeschwindigkeitsprofilen zeigt eine gute Übereinstimmung, genauso wie der angepasste Druckabfall entlang der Röhrenachse. Die Analyse der Schergeschwindigkeiten zeigt, dass der scherverdünnende Effekt des Fluids im Querschnittsbereich bei den größten Deformationen relevant wird. Tatsächlich ist das Maximum der Schergeschwindigkeit um einen Faktor 30 größer als das entsprechende Maximum bei der nichtdeformierten Röhre. Die Viskosität wird um den Faktor zwei reduziert. Der Einfluss des scherverdünnenden Verhaltens wird mit den Simulationen für ein Newtonsches Fluid verglichen.

Résumé:
Des simulations sont entreprises afin d'étudier l'écoulement d'un fluide non Newtonien rhéo-amincissant dans un tube élastique collapse, et de comparaisons sont faites avec des données expérimentales. Le fluide est modélisé au moyen de la loi de viscosité Bird-Carreau. Le domaine de calcul du tube déformé est construit à partir de données obtenues par imagerie tomographique digitale. La comparaison des champs de vitesses calculées avec les mesures de profil de vitesses par ultrason Doppler présente un bon accord, et il en est de même pour la chute de pression le long de l'axe du tube. L'analyse des vitesses de cisaillement montre que l'effet rhéo-amincissant du fluide devient important dans la section possédant la plus grande déformation. En fait, la vitesse de cisaillement maximum est à peu près un facteur trente plus grande que sa valeur correspondante dans un tube non déformé, et la viscosité est réduite d'un facteur deux. L'effet du comportement rhéo-amincissant a aussi été comparé avec des simulations identiques faites pour un fluide Newtonien.

Key words: computer simulation, computer tomography, collapsed elastic tube, OpenFOAM®, shear-thinning fluid, ultrasound Doppler velocimetry

This is an extract of the complete reprint-pdf, available at the Applied Rheology website
http://www.appliedrheology.org

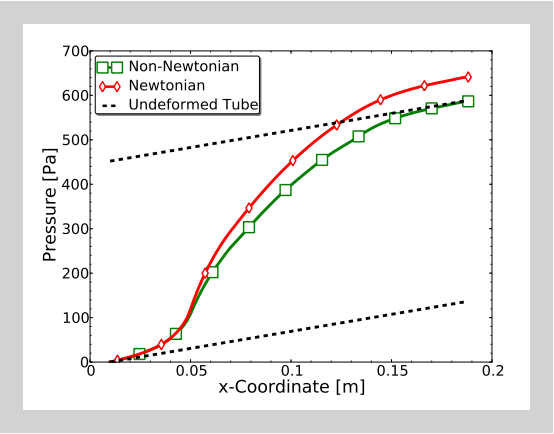

Figure 16: Pressure curves for the non-Newtonian and Newtonian simulations (The flow is from right to left).

agrees very well with the factor of 7 found in Nahar et al. [4] for the experiments, which calculated the average shear rate in the deformed tube using Equation 5, in which u_o and R were determined as follows. First, the cross-sections obtained from the tomography measurements have been approximated numerically, which allowed the determination of the average velocity u_o from the flow rate. Then, an equivalent tube radius, R, has been determined such that the equivalent circular area is equal to the one of the corresponding deformed cross-section. Using this approach, the area of the cross-section at x = 50 mm has been estimated to be A = 105.7 mm², which is a factor of 0.34 smaller than the cross-section of the undeformed tube. The excellent agreement in average shear rates between simulation and estimation confirm that the rudimentary method of determining the estimated average shear rates from the experimental data is accurate for this level of tube deformation.

As listed in Table 1, the maximum shear rate for the Newtonian case is $\dot{\gamma}_{max}$ = 647 s^{-1}, which is 4 % less than the maximum value for the non-Newtonian case. A more detailed comparison between Newtonian and non-Newtonian shear rate behavior along the cross-section x = 50 mm is shown in Figure 15. As can be seen, the shear rates of the Newtonian fluid are larger throughout most of the cross-section, except possibly at the walls. The largest difference occurs at the z-coordinate z = 9 mm, where the Newtonian shear rate is approximately 26 % higher than the non-Newtonian one. However, as is seen from Figure 2, this relatively large difference in the shear rate leads to an insignificant change in the viscosity, which explains the small differences in the velocity commented on in the previous subsection.

4.3 PRESSURE DROP COMPARISON

In the experiments, the pressure drop in the tube was measured over a distance of 910 mm, of which the middle 320 mm correspond to the deformable elastic tube, and the remaining part had a cylindrical cross-section with a radius of 10 mm. (Recall that only 180 mm of the most deformed part of the elastic tube was simulated.) The total pressure drop was measured to be 1256 Pa. The simulation pressure drop over the entire computational domain of 180 mm was 587 Pa, as can be seen from Figure 16 or Table 1. The dashed lines in this figure correspond to the theoretical pressure drop for a power-law fluid in an undeformed tube given in Equation 2. According to Bird et al. [12, page 176] this pressure drop is given by

$$\Delta p = \left(\frac{3n+1}{n}\right)^n \frac{2\kappa}{\pi^n R^{3n+1}} Q^n L \tag{6}$$

where L is the length of the tube, Q is the volumetric flow rate. Note that for a Newtonian fluid with n = 1 and $\kappa = \eta_o$ Equation 6 reduces to the Hagen-Poiseuille equation $\Delta p = 8\eta_o QL/(\pi R^4)$.

Figure 16 shows that the slope of the non-Newtonian simulation pressure curve is the steepest at x = 50 mm where the tube exhibits the largest deformation. The theoretical pressure of the non-Newtonian fluid in an undeformed tube is shown by the dashed lines at the tube inlet and outlet. These lines are tangential to the simulation curve, which is an indication that Equation 6 accurately describes the pressure gradient for the non-deformed portion of the tube. To account for the pressure discrepancy between the experiment and the simulation, the pressure drop in the remaining undeformed part of the pipe of the experiment is taken into consideration via Equation 6. The total length of this undeformed pipe is 730 mm, which leads to a pressure drop of 560 Pa, leading to a total simulation pressure drop of 1147 Pa. Given the fact that in the experiment there are several pipe connections over which the pressure drop is larger than predicted by Equation 6, the agreement between simulation and experiment is excellent. Also shown in Figure 16 is the pressure curve of the Newtonian calculation. As is seen, the pressure drop is 644 Pa (cf. Table 1), which is almost 10 % larger than for the non-Newtonian case. Since the non-Newtonian fluid under consideration is shear-thinning, its viscosity is smaller or equal to that of the Newtonian fluid. Thus, the viscous dissipation of the Newtonian fluid is larger, which accounts for the larger pressure drop.

This is an extract of the complete reprint-pdf, available at the Applied Rheology website
http://www.appliedrheology.org

5 SUMMARY AND CONCLUSIONS

The flow of a non-Newtonian fluid through a collapsed tube has been simulated using an open source CFD solver and a deformed tube geometry. The simulation results have been compared with experimental data, and additional insights have been obtained by considering local quantities for shear rates and viscosities. The geometry of the deformed tube has been reconstructed from computer tomography image analysis. The velocity profiles obtained from the simulations have been compared with corresponding ultrasound Doppler velocity profile measurements at various cross-sections. There is generally good agreement between simulation and experiment, especially given the rudimentary approximation to the geometry used in the simulation. The double peaks of the velocity profiles in the collapsed part of the tube were well reproduced. These double peaks are a consequence of the bow-tie-shaped cross-sections where the fluid follows the path of least resistance and flows fastest furthest away from the wall.

The shear-thinning effect of the fluid becomes relevant in the cross-sections with the largest deformation. The maximum shear rate is about a factor of thirty larger than its corresponding maximum value in the undeformed tube, which reduces the viscosity by a factor of two. Similarly, the average shear rate in the most deformed cross-section is a factor of 7.3 larger, which is in good agreement with the estimate derived from the experimental data. Also, the pressure drop across the tube was well predicted by the simulation after appropriate pressure corrections have been added for the non-deformed portion in the experimental setup.

In order to better assess the non-Newtonian behavior of this fluid the same flow has been simulated for a Newtonian fluid. It was found that there are significant differences in the shear rates at locations where the tube was strongly deformed, These differences are significant enough to cause sufficient shear-thinning which is reflected in the velocity profiles, and leads to a 10% increase in the pressure drop for the Newtonian fluid.

REFERENCES

[1] Marzo A, Luo XY, Bertram CD: Three-dimensional collapse and steady flow in thick-walled flexible tubes. J. Fluids Struct. 20 (2005) 817–835.

[2] Hazel AL, Heil M: Steady finite-Reynolds-number flowsin three-dimensional collapsible tubes. J. Fluids Mech. 486 (2003) 79–103.

[3] Grotberg JB, Jensen OE: Biofluidmechanics in flexible tubes. Ann. Rev. Fluid Mech. 36 (2004) 121–147.

[4] Nahar S, Jeelani SAK, Windhab EJ: Influence of elastic tube deformation on flow behavior of a shear thinning fluid. Chem. Eng. Sci. 75 (2012) 445–455.

[5] OpenFOAM®. The OpenFOAM® Foundation. http://www.openfoam.org, 2011.

[6] Takeda Y: Velocity profile measurement by ultrasound doppler shift method. Int. J. Heat Fluid Flow 7 (1986) 313–318.

[7] Nahar S, Jeelani SAK, Windhab EJ: Peristaltic flow characterization of a shear thinning fluid through an elastic tube by UVP. Appl. Rheol. 22 (2012) 43941.

[8] Kotze R, Wiklund J, Haldenwang R: Optimization of the UVP+PD rheometric method for flow behavior monitoring of industrial fluid suspensions. Appl Rheol 22 (2012) 42760.

[9] Stranzinger M: Numerical and Experimental Investigations of Newtonian and Non-Newtonian Flow in Annular Gaps with Scraper Blades. Ph.D. Thesis, Swiss Federal Institute of Technology (ETH Zurich), Diss. ETH Nr. 13369 (1999).

[10] Nahar S, Jeelani SAK, Windhab EJ: Steady and unsteady flow characteristics of a shear thinning fluid through a collapsed elastic tube. In 7th International Symposium on Ultrasonic Doppler Method for Fluid Mechanics and Fluid Engineering, Chalmers University of Technology (2010) 61–64.

[11] Patankar SV, Spalding DB: A calculation procedure for heat, mass and momentum transfer in three-dimensional parabolic flows. Inter. J. Heat Mass Transfer 15 (1972) 1787–1806.

[12] Bird RB, Armstrong RC, Hassager O: Dynamics of Polymeric Liquids, Volume 1: Fluid Mechanics. JohnWiley and Son Inc., New York (1987).

This is an extract of the complete reprint-pdf, available at the Applied Rheology website
http://www.appliedrheology.org